Modulation of lamellipodial structure and dynamics by NO-dependent phosphorylation of VASP Ser239

Susan L. Lindsay[1], Sara Ramsey[2], Michael Aitchison[2], Thomas Renné[3] and Thomas J. Evans[1,*]

[1]Division of Immunology, Infection and Inflammation, University of Glasgow, Glasgow Biomedical Research Centre, 120, University Place, Glasgow, G12 8TA, UK
[2]Department of Urology, Gartnavel General Hospital, Great Western Road, Glasgow, G12 0YN, UK
[3]Institute for Clinical Biochemistry and Pathobiochemistry, University of Würzburg, Josef-Schneider Strasse 2, 97080 Würzburg, Germany
*Author for correspondence (e-mail: t.j.evans@udcf.gla.ac.uk)

Accepted 25 June 2007
Journal of Cell Science 120, 3011-3021 Published by The Company of Biologists 2007
doi:10.1242/jcs.003061

Summary

The initial step in directed cell movement is lamellipodial protrusion, an action driven by actin polymerization. Enabled/vasodilator-stimulated phosphoprotein (Ena/VASP) family proteins are key regulators of this actin polymerization and can control lamellipodial protrusion rate. Ena/VASP proteins are substrates for modification by cyclic-nucleotide-dependent protein kinases at a number of sites. Phosphorylation of Ser239 of VASP in vitro inhibits its anti-capping and filament-bundling activity but the effects of this modification on lamellipodial structure and function are unknown. To examine the functional effects of this modification in living cells, we studied VASP phosphorylation at Ser239 by nitric oxide (NO) stimulation of cGMP-dependent protein kinase. Using live cell imaging of primary cells transfected with GFP-VASP constructs, we found that NO produced rapid retraction of lamellipodia together with cell rounding that was dependent on guanylate cyclase and type II cGMP-dependent protein kinase. In cells expressing a mutant VASP (Ser239Ala) lacking the site preferentially phosphorylated by this kinase, NO had no effect. Phosphorylation of Ser239 of VASP results in loss of lamellipodial protrusions and cell rounding, and is a powerful means of controlling directed actin polymerization within lamellipodia.

Supplementary material available online at
http://jcs.biologists.org/cgi/content/full/120/17/3011/DC1

Key words: Nitric oxide, Lamellipodia, Vasodilator-stimulated phosphoprotein

Introduction

Lamellipodial dynamics and behaviour are regulated by proteins of the Ena/VASP family, which are key controllers of actin polymerization in diverse cellular processes (Bear et al., 2000; Coppolino et al., 2001; Jay, 2000; Krause et al., 2000; Laurent et al., 1999; Lawrence and Pryzwansky, 2001; Renfranz and Beckerle, 2002; Vasioukhin and Fuchs, 2001). Lamellipodial protrusion rate is directly correlated with the amount of Ena/VASP proteins within these projections (Rottner et al., 1999). Paradoxically, Ena/VASP proteins appear to retard cell translocation, principally by promoting increased lamellipodial protrusion and turnover (Bear et al., 2000; Bear et al., 2002). The molecular basis of these effects reflects the ability of Ena/VASP proteins to act as anti-capping factors, promoting the barbed-end growth of actin filaments (Barzik et al., 2005). Additionally, these proteins also decrease the branching architecture of actin filaments, but increase actin fibre bundling (Bachmann et al., 1999; Huttelmaier et al., 1999; Laurent et al., 1999).

Cellular regulation of Ena/VASP protein function remains mysterious. These proteins are substrates for both cAMP- and cGMP-dependent protein kinases (PKA and PKG, respectively) (Butt et al., 1994). VASP has three PKA/PKG phosphorylation sites (Krause et al., 2003): Ser157, Ser239 and Thr278 (residue numbers apply to human VASP). Ser157 is the preferred site of phosphorylation by PKA (Butt et al., 1994; Lambrechts et al., 2000) and is conserved within all vertebrate Ena/VASP proteins. Ser239, adjacent to the G-actin-binding site, is preferentially phosphorylated by PKG (Butt et al., 1994). Thr278 is phosphorylated by AMP-activated protein kinase (Blume et al., 2007). The cellular effects of VASP-phosphorylation have remained obscure. Most studies have focused on in vitro phosphorylation of Ena/VASP proteins and how this affects ligand binding and actin polymerization. Ser157 phosphorylation seems to correlate with activation of Ena/VASP proteins, although studies using different technologies have come to opposite conclusions about the effect of PKA on F-actin binding and bundling activity (Harbeck et al., 2000; Laurent et al., 1999). PKA phosphorylation correlates with filopodia formation in neurons (Lebrand et al., 2004) and phosphorylation sites are crucial to Ena/VASP function in cell migration (Loureiro et al., 2002). Analysis of the role of Ser239 phosphorylation within the EVH2 domain suggests that at least in vitro, phosphorylation at this site reduces VASP's actin anti-capping and filament bundling activity (Barzik et al., 2005) and interferes with actin fibre formation (Zhuang et al., 2004). The specific effects of phosphorylation at this site on lamellipodial dynamics remain unknown. Since nitric oxide (NO) has been shown to trigger phosphorylation of Ser239 of VASP (Oelze et al., 2000), we set out to explore the effects of NO-dependent phosphorylation of VASP on its function in human primary renal tubule epithelial cells (PTECs) and embryonic keratinocytes (HEKs).

Results

VASP within resting epithelial cells

We examined the effects of NO-dependent phosphorylation of VASP on its function in human primary renal tubule epithelial cells (PTECs). These cells are motile epithelial cells that make abundant NO following cytokine treatment (Glynne et al., 2001). These cells express VASP, which is particularly concentrated in the leading edge of lamellipodia and also in focal adhesions (Fig. 1a), as previously described (Reinhard et al., 1992). To study the dynamic behaviour of VASP within the lamellipodia, we constructed an expression plasmid of VASP fused to the C-terminus of GFP [wild-type (WT) GFP-VASP] and used this to transfect human PTECs. We also constructed a mutant VASP containing a point mutation of serine at position 239 to alanine (S239A) – Ser239 being the major site for cGMP-dependent kinase mediated phosphorylation – and also fused this to GFP in the same manner (S239A GFP-VASP). Both GFP-VASP constructs showed identical localization to that seen in untransfected cells (Fig. 1b,c). There was no difference in the subcellular distribution of WT GFP-VASP compared with S239A GFP-VASP (Fig. 1b,c). Expression levels of the transfected WT and S239A GFP-VASP constructs were virtually identical, as judged both by fluorescence imaging and immunoblotting (Fig. 1d). Control imaging of cells transfected with GFP alone (Fig. 1e) showed homogenous cytoplasmic staining and cells transfected with empty vector showed no fluorescent staining (Fig. 1e), confirming that the observed distribution of GFP-VASP was specific.

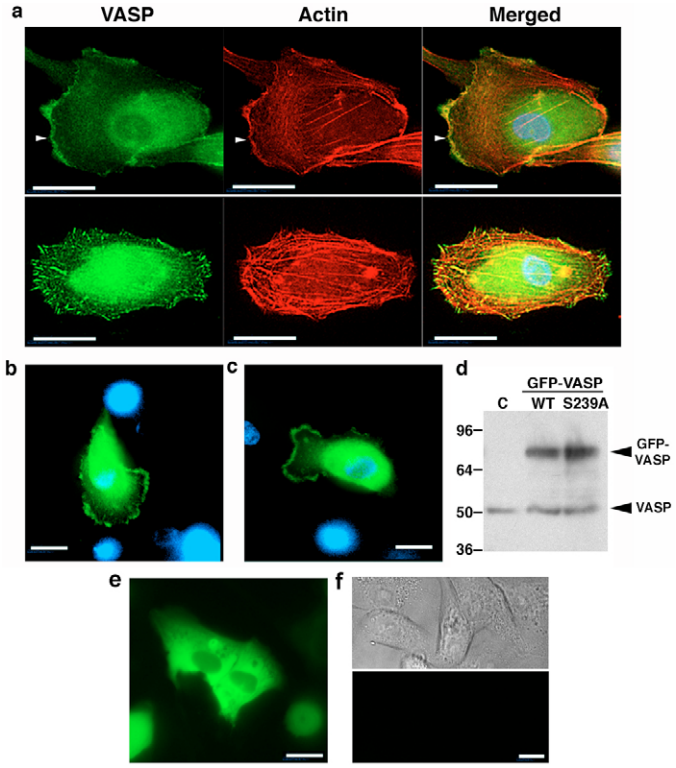

Fig. 1. Distribution of VASP within human PTECs. (a) Cells stained for VASP (green), actin (red) or merged with images of nuclei stained with DAPI (blue). The arrowhead in the upper panel indicates the edge of a lamellipodium. (b,c) Human PTECs were transfected with WT GFP-VASP (b) or GFP-S239A VASP (c), then fixed 16 hours after transfection and imaged for GFP (green) and nuclei stained with DAPI (blue). (d) Western blot of cell extracts from human PTECs either untransfected control (C) or transfected with WT GFP-VASP (WT) or S239A GFP-VASP (S239A). Molecular mass markers (kDa) are to the left of the panel. Arrowheads indicate bands of endogenous VASP (~50 kDa) and GFP-VASP fusion proteins (~75 kDa). The usual doublet band of VASP is not seen on this gel as it was optimized to show both endogenous and transfected protein. (e) Human PTECs transfected with a GFP control vector alone. (f) Untransfected human PTECs visualised using phase-contrast microscopy (upper panel) or GFP fluorescence (lower panel). Bars, 10 μm.

Live cell imaging allowed us to follow the dynamic changes in cell behaviour and VASP distribution within lamellipodia. Localized concentration of VASP at the edge of the cell correlated with projection of that part of the membrane (Fig. 2a and supplementary material Movie 1). The movie also shows the concentration of VASP within membrane ruffles, which appear to move back from the leading edge of the membrane. Some lamellipodia were a persistent broad front at the leading edge of the cell (Fig. 2a); others were more transient and were extended in directions other than the principal axis of movement (Fig. 2b). Analysis of time-lapse sequences and kymography (Fig. 2c,d) were used to derive the rates of cell movement and lamellipodial protrusion (Fig. 2i), with median values of 0.37 and 0.24 $\mu m\ min^{-1}$, respectively. Similar rates of cell movement are reported for other cells, e.g. 0.5 $\mu m\ min^{-1}$ for human epidermal keratinocytes (Hinz et al., 1999), although lamellipodial protrusion velocity in these and other cells was rather higher.

In human PTECs transfected with S239A GFP-VASP, there was no difference in the distribution of VASP in resting cells (Fig. 2e-h and supplementary material Movie 2). Quantification of rates of cell movement and lamellipodial protrusion showed no significant differences between cells transfected with WT or S239A GFP-VASP (Fig. 2i).

Effects of NO on VASP within lamellipodia

Next, we examined the behaviour of the WT and mutant GFP-VASP construct following addition of an NO donor that we expected to phosphorylate WT VASP at the Ser239 site. In resting cells, Ser239 phosphorylation of VASP was undetectable (Fig. 3a), although about 30% of the protein was phosphorylated at Ser157, as judged by the lesser mobility (50 kDa compared with 46 kDa) on SDS PAGE produced by phosphorylation at this site (Butt et al., 1994) and quantified by digital scanning of gel images (Fig. 3b). Following addition of NO donor, there was a rapid phosphorylation of VASP at Ser239, which was readily detectable between 5 and 10 minutes after NO donor addition (Fig. 3a). Nonspecific binding to immunoglobulin is indicated by an asterix above the band of phosphorylated VASP. Since optimal separation from this band did not give very clear separation of the 50 kDa and 46 kDa forms of VASP, we assayed the effects of NO donors on phosphorylation of Ser157 VASP on separate gels. NO donors did not produce any significant difference to Ser157 phosphorylation in these cells, as judged by the lack of any significant change in the proportion of the 46 kDa and 50 kDa forms of VASP (Fig. 3b).

Following addition of NO donor to these cells, we observed

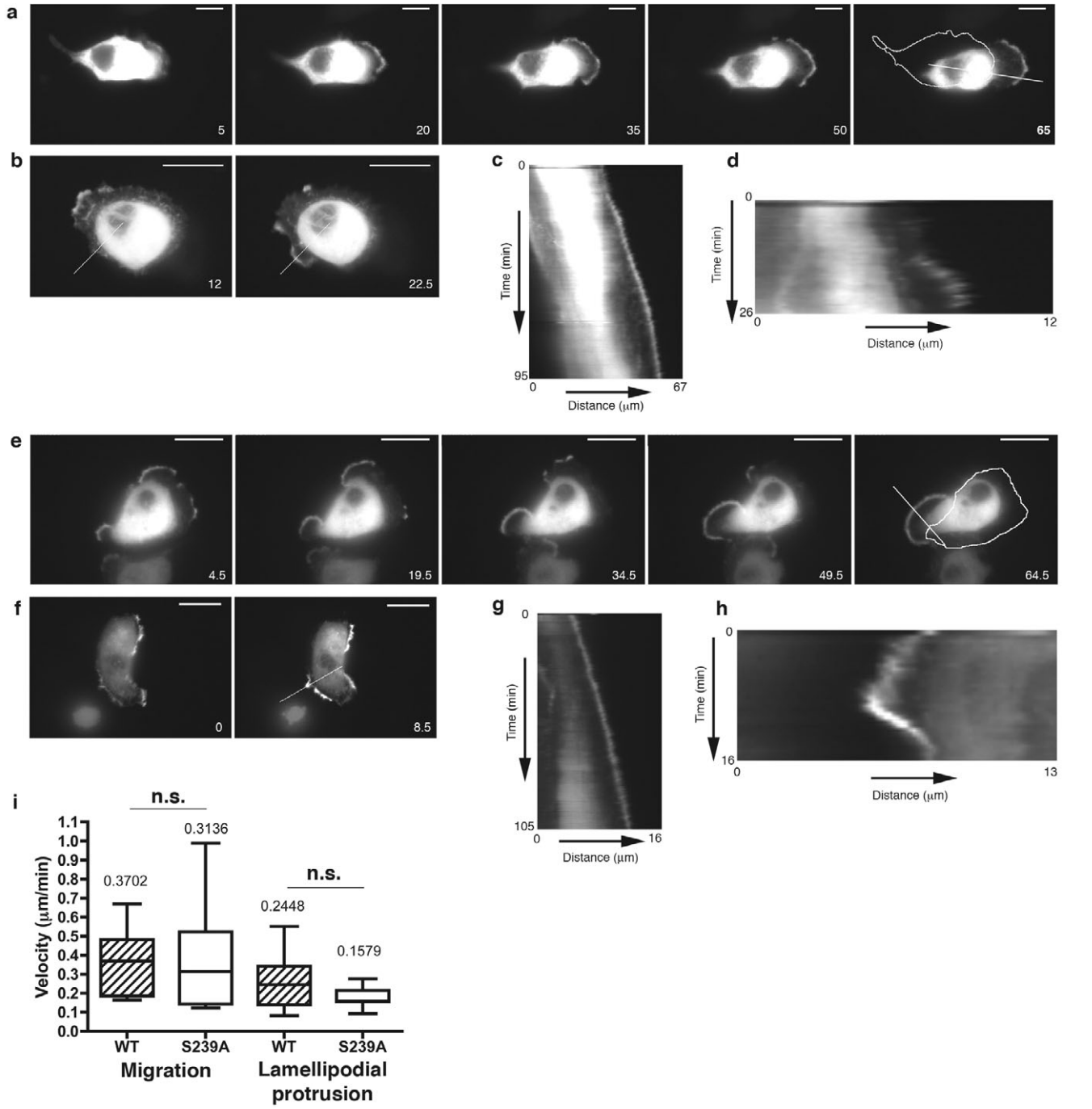

Fig. 2. Movement of human PTECs transfected with GFP-VASP and GFP-S239AVASP. (a) Sequence of frames taken from Movie 1 (see supplementary material), showing one cell imaged at the indicated intervals (in minutes). The final frame (t=65 minutes) shows the outline of the original cell at its starting position at t=0 minutes. The white line indicates the axis used to generate the kymograph in panel c. (b) Still frames from another cell transfected with WT GFP-VASP and imaged at the indicated times (in minutes) after the start of the experiment. The white line indicates the axis used to generate the kymograph in panel d. (c) Kymograph of the cell shown in panels a, taken along the axis indicated by the white line. (d) Kymograph of the cell shown in panels b, taken along the axis indicated by the white line. (e) Sequence of frames from Movie 2 (see supplementary material), showing one cell imaged at the indicated intervals (in minutes). The final frame (t=64.5 minutes) shown the outline of the original cell at its starting position at t=0 minutes. The white line indicates the axis used to generate the kymograph in panel g. (f) Still frames from another cell transfected with S239A GFP-VASP and imaged at the indicated times (in minutes) after the start of the experiment. The white line indicates the axis used to generate the kymograph in panel h. (g) Kymograph of the cell in shown panels e, taken along the axis indicated by the white line. (h) Kymograph of the cell shown in panels f, taken along the axis indicated by the white line. Bars, 10 μm. (i) Box and whisker plot of cell migration and lamellipodial projection speeds for human PTECs transfected with WT GFP-VASP and S239A GFP-VASP (WT and S239A, respectively). Horizontal line is the median value, the box encloses the 25th and 75th percentiles. The bars indicate the range of the values. The differences in cell migration and lamellipodial projection speeds between WT and S239A were not significant (n.s.) as determined by Mann-Whitney test; n=7-12 independent observations.

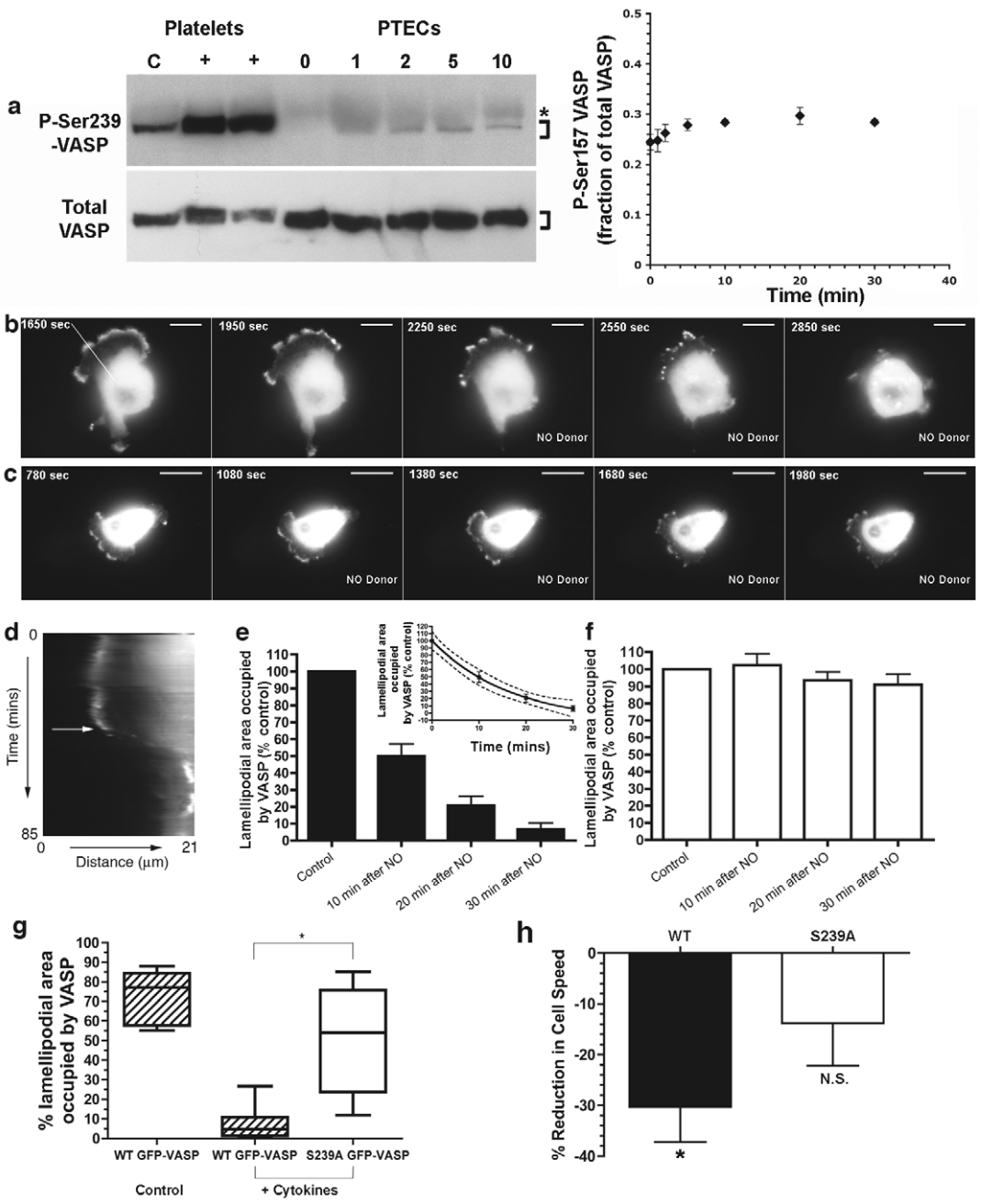

Fig. 3. Effect of NO on VASP and lamellipodial dynamics. (a) Western blot showing Ser239-phosphorylation status of VASP at various times (in minutes) after the addition of NO donor. VASP proteins are indicted by square brackets at the right of the gel. VASP was immunoprecipitated from human PTECs and analysed for the presence of VASP phosphorylated at Ser239 (P-Ser239-VASP) (upper panel). The blot was then stripped and reprobed for total VASP (lower panel). Immunoprecipitates from untreated positive-control (C) and NO-treated (+) platelets are shown in the first three lanes from the left. Control immunoprecipitates with control immunoglobulin at 30 minutes after addition of NO donor showed no VASP (data not shown). The experiment was repeated three times with similar results. The fraction of VASP phosphorylated at Ser157 following addition of NO donor was calculated as described in Materials and Methods and is plotted in the diagram on the right. Values are the means of duplicates; error bars are ± s.e.m. (b,c) Sequence of frames taken from time-lapse Movie 3 (see supplementary material), showing one human PTECl transfected with (b) WT GFP-VASP or (c) S239A GFP-VASP and treated with NO donor. Frames were taken at the indicated times. NO donor was added at 2250 seconds for panels b, and at 1080 seconds for panels c. Bars is 10 μm. The white line in the first panel of b indicates the axis used to generate the kymograph in d. (d) Kymograph of the cell shown in panels b, taken along the axis indicated by the white line. (e) Effects of NO on the localization of VASP in lamellipodia. The area of lamellipodia occupied by WT GFP-VASP was calculated just prior to (control) and after the addition of NO donor at the times indicated, and are expressed as a percentage of the control value prior to NO addition. Values are the means ± s.e.m.; n= 12. The effect of NO was significant as determined by ANOVA, P<0.0001. The diagram in the inset shows an exponential decay curve fitted to the data; dotted lines are 95% confidence limits. The calculated half-life of reduction of VASP localization within lamellipodia after NO addition was 12.6 ± 0.45 minutes (± s.e.m.). (f) Data from experiment as described for panel e, but from cells transfected with S239A GFP-VASP. No significant effect after the addition of NO donor was observed (ANOVA, P=0.2461). Values are the mean ± s.e.m.; n= 13. (g) GFP-VASP distribution in lamellipodia following induction of iNOS with cytokines for 16 hours. Box indicates the 25th to 75th percentiles of the percentage of lamellipodial area occupied by VASP, the line the median value and the bars the range. Hatched bars show data of WT GFP-VASP (n=11), white bars of S239A GFP-VASP (n=6) after the treatment as indicated. Difference between the median values of WT and S239A GFP-VASP following cytokine stimulation is significant (*P=0.0022, Mann-Whitney test). (h) Percentage change in mean speed of cells following addition of NO donor. Bars show mean speed of cell centroids (calculated as described in the Materials and Methods) for 20 minutes, following addition of NO donor to WT GFP-VASP (n=8) and S239A GFP-VASP (n=8); bars are ± 1 s.e.m. *P=0.0033 significantly different from no change (one sample t-test); N.S. not significant difference from no change.

profound changes in cell shape and the distribution of WT VASP within lamellipodia (Fig. 3b and supplementary material Movie 3). First, the NO donor produced a dramatic removal of WT VASP from the cell edge, such that after 30 minutes treatment virtually no VASP remained at this site (supplementary material Movie 3 and Fig. 3b). Secondly, NO produced a withdrawal of the edge of the cell, retraction of all cellular processes and cell rounding (supplementary material Movie 3 and Fig. 3b). A kymograph of this retraction is shown in Fig. 3d, which shows that the cell edge retracted with a velocity of 0.99 μm min^{-1}. In cells transfected with S239A GFP-VASP, the NO donor was without effect, with no significant removal of VASP from the lamellipodial edge (Fig. 3c and supplementary material Movie 4). We quantified these changes, and showed that the amount of WT VASP localized to the lamellipodial edge declined significantly following NO addition (Fig. 3e, $P<0.0001$, ANOVA), with a half-life of 11.57 minutes (Fig. 3e, insert). In cells transfected with S239A GFP-VASP, there was no significant decline in the amount of VASP localized to the lamellipodial edge (Fig. 3f).

Human PTECs do not express constitutive NO synthases, but do express inducible NO synthase (iNOS) following exposure to pro-inflammatory cytokines (Glynne et al., 2001). In order to test the effect of endogenous NO production within these cells, we stimulated human PTECs transfected with either WT GFP-VASP or S239A GFP-VASP for 16 hours with cytokines and then measured the percentage of lamellipodial area occupied by VASP (Fig. 3g). Following this stimulation, very little WT GFP-VASP was detected in lamellipodia but, by contrast, the median amount of S239A GFP-VASP within lamellipodia remained at a significantly higher level (Fig. 3g, $P=0.0022$, Mann-Whitney test). Thus, endogenous NO production has an effect on VASP similar to that of an NO donor, and this effect was abrogated in the S239A GFP-VASP mutant.

NO donors in these cells do not produce detectable cytotoxicity in this time frame (Glynne et al., 2001) (data not shown), although they do induce cell shedding after 24 hours (Glynne et al., 2001). Additionally, the lack of effect of NO donor on cells transfected with S239 GFP-VASP stresses the crucial importance of Ser239 phosphorylation as the basis for the observed changes.

The removal of VASP from lamallipodia following treatment with NO donor suggested this should produce alterations in cell movement, because most cells move by extension of the leading edge lamellipodium. We measured cell speeds in human PTECs transfected with WT or S239 GFP-VASP. Following addition of NO donor, there was a ~30% reduction in average cell speed in cells transfected with WT GFP-VASP, a significant reduction (Fig. 3h). By contrast, in cells transfected with S239A GFP-VASP, there was only a small, not statistically significant, reduction in cell speed following NO addition (Fig. 3h). Thus, loss of VASP from the leading edge of the cell after NO addition leads to a reduction in cell speed.

The retraction of the cell edge following treatment with NO donor led to considerable changes in cell shape which we quantified by measuring changes in total cell area. In our time-lapse imaging we also recorded the phase-contrast view of each cell at the same time as the signal from the WT GFP-VASP (Fig. 4a). This showed the edge of the cell (arrow heads) correlating with the presence of the WT GFP-VASP. In cells

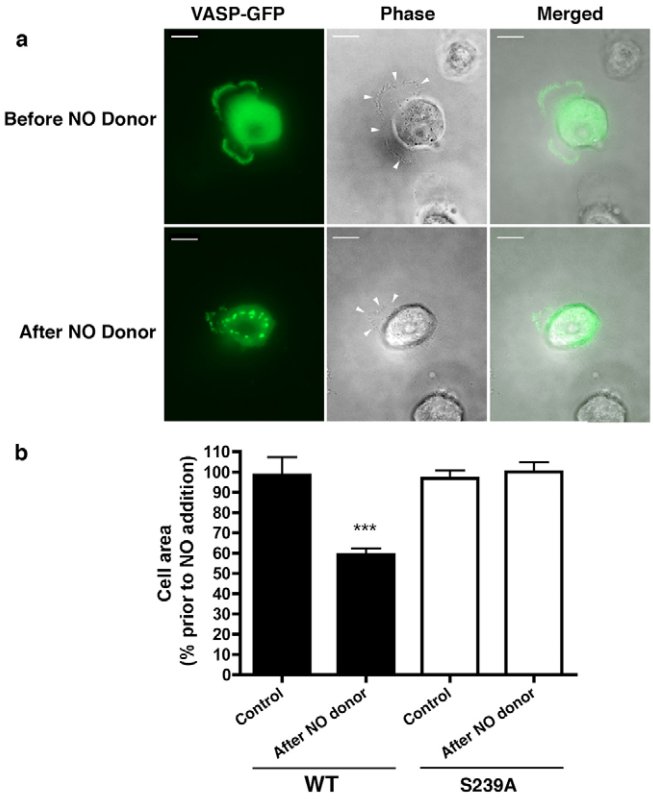

Fig. 4. Influence of VASP phosphorylation on cell area after the addition of NO donor. (a) Sequence of frames taken from Movie 1 (see supplementary material), showing distribution of WT GFP-VASP (green) in transfected human PTEC before (t=0 minutes) and after (t=30 minutes) addition of NO donor. The outline of the cells is shown in the phase-contrast micrographs. Merged images are on the right. Bars, 10 μm. Arrowheads mark edge of cell. (b) Mean cell area normalized to that just prior to addition of NO donor. Black bars, cells transfected with WT GFP-VASP; white bars cells transfected with S239A GFP-VASP. Areas were measured 30 minutes before (Control) and after (After NO donor) NO donor addition. Values are the mean ± s.e.m.; n=12 or more. Reduction in area in cells transfected with WT GFP-VASP following NO donor addition was significantly reduced compared with control value ($P<0.01$, two-tailed t-test).

expressing WT GFP-VASP, 30 minutes after NO addition, the total cell area was reduced to just under 60% of the value observed immediately before NO addition (Fig. 4b), a significant reduction ($P<0.01$, two-tailed t-test). The aggregation of VASP after NO addition noticed here was not a consistent feature following NO donor addition. By contrast, cells transfected with the S239A GFP-VASP mutant showed no significant change in cell shape over the same time period (Fig. 4b). Thus, S239A GFP-VASP following NO treatment remains constitutively active compared with WT GFP-VASP.

The NO donor produced a steady decline in lamellipodial VASP over a 30-minute period, associated with persistent cell rounding (Figs 3 and 4). We were not able to follow cells reliably after this time to study potential recovery but, on those occasions when we were able to image cells for prolonged periods, there was no recovery of VASP distribution or cell shape in WT GFP-VASP after a 60-minute period and cells

transfected with S239A GFP-VASP retained their normal appearance (data not shown).

Effects of NO on lamellipodia and cell shape in HEKs

We repeated our studies of the behaviour of WT GFP-VASP and S239A GFP-VASP in a different primary human cell, embryonic keratinocytes (HEKs). Following addition of NO, very similar changes in amount of VASP within lamellipodia and reduction of cell area were seen in cells transfected with WT GFP-VASP (Fig. 5a). These changes were absent in cells transfected with S239A GFP-VASP (Fig. 5b). We quantified these changes as decribed for PTECs and found a significant decline in the amount of WT GFP-VASP localized to the retracting cell edge following NO addition, with a half-life of 18.6 minutes (Fig. 5c). No significant decline in the amount of VASP at the lamellipodial edge was seen in cells transfected with S239A GFP-VASP (Fig. 5d). In addition, there was a significant reduction in cell area following NO treatment in cells transfected with WT GFP-VASP that was not seen with the S239A mutant (Fig. 5e). Thus, the critical dependence of VASP Ser239 phosphorylation on the disappearance of VASP from lamellipodia and reduction in cell area in HEKs following NO treatment was comparable with that found in PTECs.

Effects of the phosphomimetic S239D VASP mutation

Given the observed effects of NO on VASP distribution that are dependent on Ser239, we predicted that a phosphomimetic mutation at this site (S239D) should also produce differences in VASP localization within lamellipodia. We transfected human PTECs with a GFP-tagged VASP construct bearing this mutation (S239D GFP-VASP) and analysed the distribution of this mutant VASP (Fig. 6). In contrast to the uniform presence of WT VASP within lamellipodia (Fig. 6a), the S239D GFP-VASP mutant was only found within about 12% of lamellipodia (Fig. 6b). Cells expressing the mutant did not, however, show any rounding (Fig. 6a), suggesting that endogenous VASP maintained normal cell architecture.

Role of guanylate cyclase and type II cGMP-dependent protein kinase in mediating the effects of NO on lamellipodia

We assayed whether inhibition of cGMP-dependent protein kinases or interruption of production of cGMP from guanylate cyclase has any effects on the NO-triggered changes of human PTEC lamellipodia and cell shape. We used small interfering RNA (siRNA) to downregulate the expression of PKG type I and type II (PKG I and PKG II, respectively) in human PTECs (Pfeifer et al., 1996; Pfeifer et al., 1998). Downregulation of PKG I was without effect on the decline in WT GFP-VASP localization and changes in cell shape following addition of NO donor (Fig. 7a and supplementary material Movie 5). Kymographic analysis showed clearly the retraction of the cell

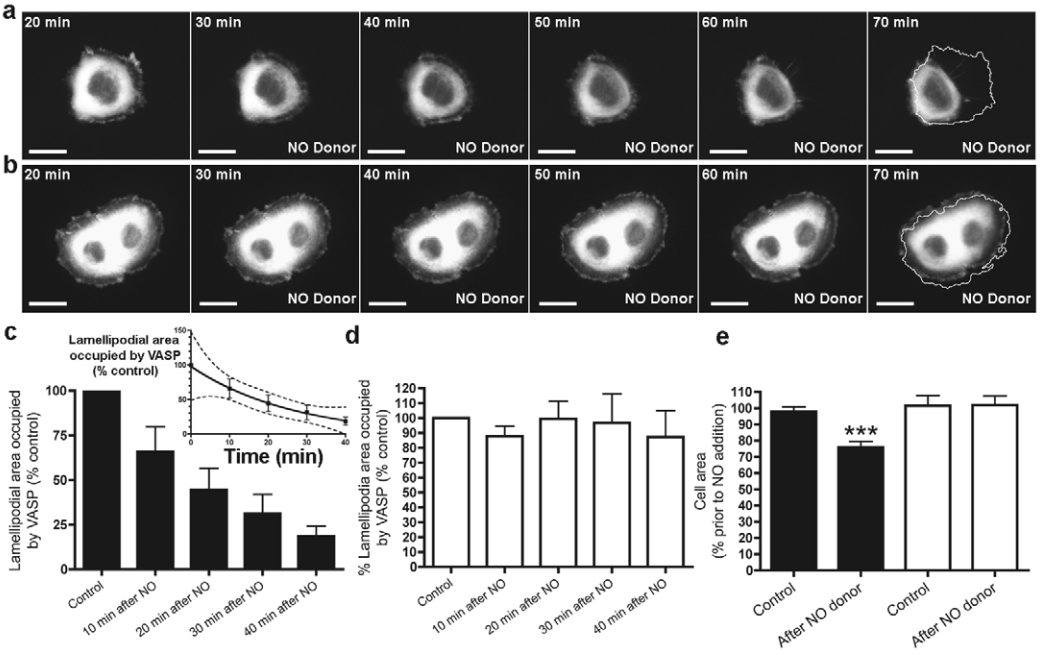

Fig. 5. Effects of NO on lamellipodial VASP and cell shape in human embryonic fibroblasts (HEK cells). (a,b) Montage from time-lapse sequence of HEK cells transfected with WT GFP-VASP and S239A GFP-VASP respectively at the indicated times. NO donor was added at 25 minutes in panel a and 24 minutes in panel b. Last panel shows outline of cell from first panel. (c) Effects of NO on the localization of VASP in lamellipodia. The area of lamellipodia occupied by WT GFP-VASP was calculated just prior to addition of NO donor (control) and at the indicated times after NO addition, expressed as a percentage of the control value prior to NO addition. Values are the mean ± s.e.m.; n=7. The effect of NO was significant as determined by ANOVA, P<0.001. The inset shows an exponential decay curve fitted to the data; dotted lines are 95% confidence limits. The calculated half-life of reduction of VASP localization within lamellipodia after NO addition was 18.6 minutes. (d) As panel c, but from cells transfected with S239A GFP-VASP. No significant effect after NO donor addition was observed (ANOVA, P=0.32). Values are the mean ± s.e.m.; n=6. (e) Mean cell area normalized to that just prior to NO donor addition. Black bars, cells transfected with WT GFP-VASP, white bars cells transfected with S239A GFP-VASP. Areas were measured 30 minutes before (Control) and after (After NO donor) NO donor addition. Values are the mean ± s.e.m.; n=6. Decrease of area in cells transfected with WT GFP-VASP following NO donor addition was significantly reduced compared with control value (***P<0.001, two-tailed t-test).

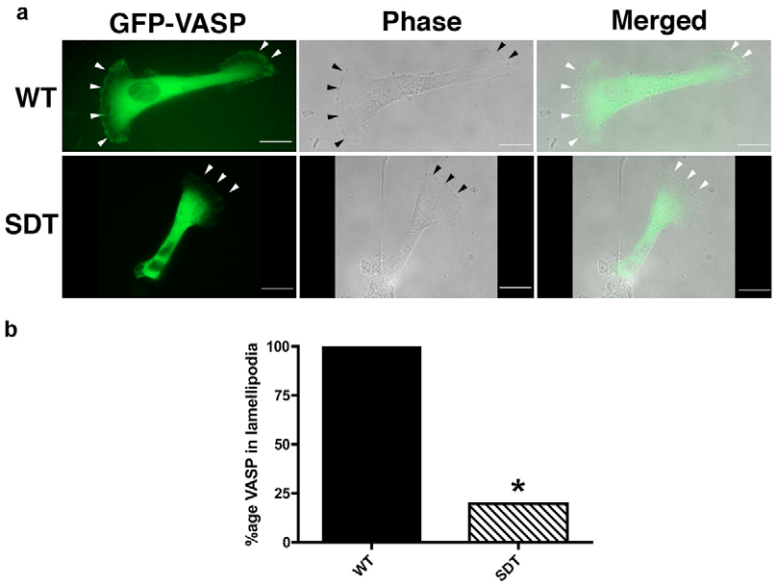

Fig. 6. Effects of the phosphomimetic S239D mutation on VASP distribution. (a) Distribution of WT GFP-VASP and S239D GFP-VASP fusions (green) in human PTECs with corresponding phase-contrast views. Edges of lamellipodia are shown by arrowheads. Bar is 10 μm. (b) Quantification of VASP in lamellipodia. Percentage of lamellipodia containing VASP measured as described in the Materials and Methods for WT GFP-VASP (WT; n=30) and S239D GFP-VASP (SDT; n=61). *P<0.0001 (Fisher's exact test), significant difference from WT GFP-VASP.

edge following addition of NO donor (Fig. 7b). Analysis of data from a number of cells showed that WT GFP-VASP was removed from the lamellipodial edge with a half-life of 10.13 minutes following addition of NO donor in cells treated with siRNA targeting PKG I (Fig. 7e,h), virtually identical kinetics to those seen in cells in which PKG I was not downregulated (Fig. 7h and compare Fig. 3e). Similarly, reduction of PKG I levels was without effect on the reduction in cell area following addition of NO donor to human PTECs (Fig. 6g).

By contrast, we found that reduction in PKG II levels prevented any effect of NO on the cells (Fig. 7c,d). Thus, in cells transfected with WT GFP-VASP, downregulation of PKG II prevented both the reduction in VASP localization to lamellipodia (Fig. 7f and Movie 6) and the reduction in cell area (Fig. 7g). Thus, we concluded that type II PKG was required to mediate the effects of NO on VASP.

Following addition of NO donor, cGMP levels are elevated by the action of the NO-sensitive guanylate cyclase (Hofmann et al., 2000). This is specifically inhibited by the drug 1H-[1,2,4]oxadiazole [4,3-a]quinoxalin-1-one (ODQ) (Lee et al., 2000). Following ODQ treatment for 30 minutes, there was a small but not significant reduction in the amount of VASP localized to the lamellipodial edge (Fig. 7i). Addition of NO donor produced no further decrease in VASP localization to the lamellipodial edge, nor did it alter cell shape following addition of NO donor (Fig. 7j). Thus, the effects of NO on VASP and cell shape are inhibited by ODQ, suggesting that the generation of cGMP through guanylate cyclase is required.

Effects of NO on the actin cytoskeleton

Staining of cells for filamentous actin with fluorescent phalloidin showed that following treatment with NO donor the changes in VASP distribution were paralleled by alterations in actin distribution. Compared with untreated control cells (Fig. 8a), filamentous actin within lamelliopodia was virtually abolished (Fig. 8b), although occasionally cells showed an intact cortical actin cytoskeleton. As noticed in live cell imaging, following treatment with NO donor, cells tended to round up and appear smaller (Fig. 8b). However, there was little change in VASP within focal adhesions following addition of NO donor (Fig. 8c), in agreement with previous reports, which found no effect of phosphorylation of VASP on its localization to focal adhesions unless all three possible phosphorylation sites were mutated (Smolenski et al., 2000).

Discussion

Our work identifies for the first time an important functional consequence of PKG phosphorylation of VASP Ser239 on lamellipodia. Phosphorylation at this amino acid residue results in the rapid loss of VASP from lamellipodia, which are withdrawn into the cell leading to cell rounding. We propose that NO and other mediators of changes in cGMP levels are, thus, regulators of VASP function and can produce alterations in actin-rich cellular protrusions, such as the lamellipodia studied here. This provides a powerful means of controlling lamellipodial dynamics and, hence, potentially altering directed cell movement. Three sets of observations reported here support this hypothesis. First, treatment of primary human epithelial cells and embryonic keratinocytes with a NO donor results in loss of VASP from the lamellipodial edge, retraction of the lamellipodia and cell rounding. These changes were all prevented in cells transfected with a mutant VASP in which the Ser239 phosphorylation site had been mutated to Ala239 and mimicked by cells expressing the S239D phosphomimetic VASP mutant S239D GFP-VASP. Second, we demonstrate that the NO-induced alterations are dependent on PKG II and guanylate cyclase, consistent with the generation of cGMP following NO donor treatment and the subsequent activation of PKG following phosphorylation of VASP Ser239. Third, in cells treated with cytokines to induce endogenous NO production, loss of VASP from the lamellipodial edge was again entirely dependent on the presence of Ser239. Taken together, these data strongly support an important role for phosphorylation of VASP Ser239 in controlling lamellipodial structure and function.

Understanding how actin polymerization is controlled is of central importance in many cellular functions. Control of this polymerization is essential in changing cell behaviour, such as

from a motile to non-motile phenotype, or changing cell direction during chemotaxis (Bretschneider et al., 2004; Diez et al., 2005). Ena/VASP family proteins are crucial in directing actin polymerization, but since these proteins are constitutively present within cells, a means must exist to control their activity. Phosphorylation is an attractive method of control that is rapid and can be tightly regulated.

All Ena/VASP members share a common tripartite structure with an N-terminal Ena/VASP homology 1 (EVH1) domain, a central proline-rich region and a C-terminal EVH2 domain. The EVH1 domain binds to proteins with a poly-proline II helix, such as vinculin and zyxin, that directs Ena/VASP proteins to focal complexes and adhesions. The central proline-rich core binds to the G-actin-binding protein profilin, as well

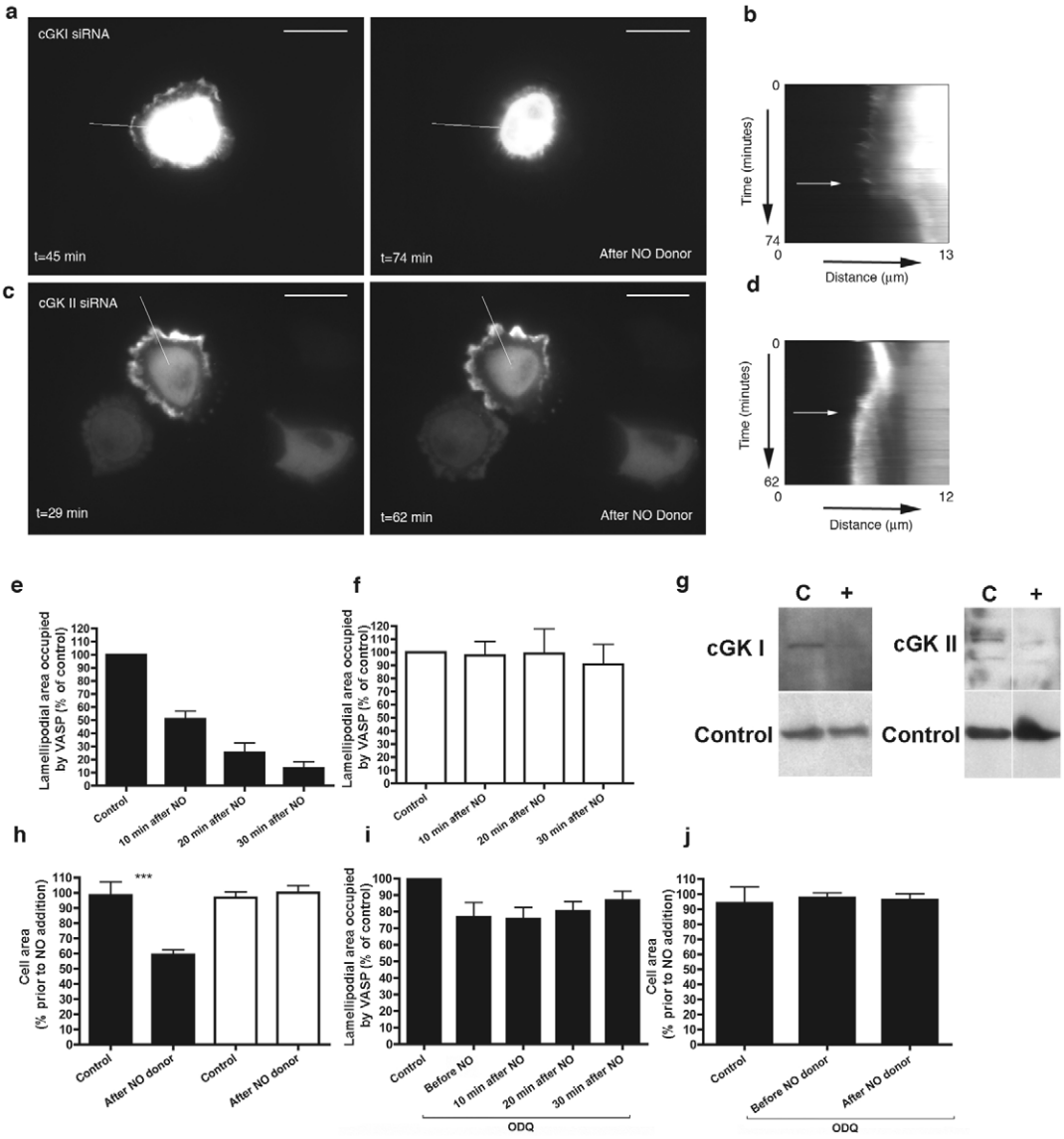

Fig. 7. Dependence of NO effects on PKG I and PKG II and guanylate cyclase. (a,c) Distribution of WT GFP-VASP in human PTEC co-transfected with siRNA targeting (a) PKG I or (c) PKG II (supplementary material Movies 5 or 6, respectively). Montage of cell images taken immediately before (left panels) and after (right panels) addition of NO donor, showing distribution of WT GFP-VASP. Time points at which images were taken are shown in each panel. White lines in each image show the axises used to generate the kymographs shown in b and d. Bars, 10 μm. (b and d) Kymographs of the cell in panels a and c, respectively, using the axis as shown. Arrows indicate the time at which the NO donor was added. (e,f) Localization of WT GFP-VASP within lamellipodia of cells co-transfected with siRNA targeting (e) PKG I or (f) PKG II, measured as a percentage of the value immediately before addition of NO donor (control=100%). Values are the mean ± s.e.m. at the indicated times after addition of NO donor; n=8 (PKG I) and n=10 (PKG II) separate determinations. The change in percentage of WT GFP-VASP within lamellipodia in response to NO donor addition was significant for cells transfected with siRNA targeting PKG I (P<0.0001, ANOVA) but not for siRNA targeting PKG II (P=0.8841, ANOVA). (g) Effect of the siRNA on PKGI or PKG II protein levels in cells transfected with control siRNA (C) or siRNAs specifically targeting the indicated PKG isoforms (+). Loading control (actin) is shown in the lower panel. (h) Change in cell area following addition of NO donor to cells transfected with siRNA targeting PKG I (black bars) or PKG II (white bars). Values were determined as described for Fig. 4b. Results are given as the mean ± s.e.m.; n=13 (PKG I) and n=11 (PKG II) individual determinations. The difference between the area after addition of NO donor in PKG I transfected cells was significantly reduced by NO addition (***P<0.01, two-tailed t-test). (i) Localization of WT GFP-VASP within lamellipodia of cells treated with ODQ, measured as a percentage of the value immediately before addition of NO donor (control=100%). Addition of ODQ for 30 minutes produced a small and non-significant decline in WT GFP-VASP within lamellipodia. Values are the mean ± s.e.m. at the indicated times after addition of NO donor of six separate determinations. The change in percentage of WT GFP-VASP within lamellipodia in response to NO donor was not significant for cells treated with ODQ (P>0.05, ANOVA). (j) Change in cell area following addition of NO donor to cells treated with ODQ. Values were determined as described for Fig. 4b. Results are mean ± s.e.m.; n=6. The difference between the area after NO addition in ODQ treated cells was not significant (P>0.05, two-tailed t-test).

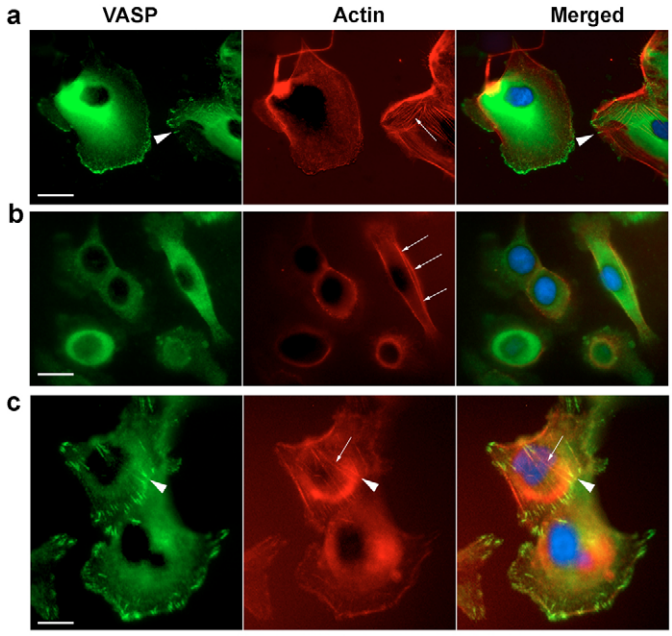

Fig. 8. Effects of NO on F-actin and focal adhesions in PTECs. (a) Untreated cells stained for VASP (green), actin (red) and nuclei (blue). Arrowheads indicate focal adhesions, arrows indicate actin stress fibres. (b) Changes in F-actin/VASP in cells following addition of NO donor and the effects on lamellipodia. After 30-minute treatment with NO donor, cells were fixed and stained for VASP (green), actin (red) and nuclei (blue). Cellular actin was not seen in cell processes. Occasionally, cells retained a cortical actin cytoskeleton (arrows). (c) Changes in F-actin/VASP in cells following addition of NO donor and the effects on focal adhesions. Cells treated and stained as described for panel b. This panel shows specifically cells with focal adhesions (arrowheads) or actin stress fibres (arrow) that show no effect following treatment with NO donor. Bars, 10 μm.

as to a number of proteins containing SH3 and WW domains. The EVH2 domain binds both G- and F-actin, as well as containing a coiled-coil motif that is essential for Ena/VASP oligomerization. The Ser239 studied here is located immediately adjacent to the G-actin-binding site and biochemical data suggest that the anti-capping and filament-bundling activities of VASP are inhibited by phosphorylation at this site (Barzik et al., 2005). However, Ena/VASP proteins are also essential for filopodial production (Mejillano et al., 2004), which may account for the lack of these processes in cells treated with NO donor. Ser239 phosphorylation also inhibits actin-fibre formation (Zhuang et al., 2004). The exact physicochemical effects of Ser239 phosphorylation, however, requires further analysis as not all studies have found that VASP antagonises actin-capping proteins (Samarin et al., 2003; Schirenbeck et al., 2006).

Loss of VASP localization at lamellipodia after its phosphorylation at Ser239 might also indicate a crucial importance of this residue in the interaction of VASP with scaffolding proteins, such as lamellipodin, that appear to direct VASP to the lamellipodial edge (Krause et al., 2004). Such interactions might be important in linking environmental cues to changes in cell behaviour controlled by VASP and actin polymerization. NO can play an important role in such changes in cell locomotion, for example, in osteoclasts (Yaroslavskiy et al., 2005) and endothelial cells (Smolenski et al., 2000). NO and cGMP changes are also important in controlling neuronal development (Bicker, 2005; Haase and Bicker, 2003). The effects of NO on cell motility are complex: in endothelial cells PKG I activation inhibits cell motility (Smolenski et al., 2000), although another study found that NO supports endothelial cell migration (Murohara et al., 1999). Movement requires a coordinated cycle of adhesion and detachment, and endogenous NO effects within living cells might be subject to rapid changes that allow cycles of lamellipodial extension and retraction. We found that NO-mediated phosphorylation of VASP at Ser239 was associated with a reduction in cell speed (Fig. 3h), as might be expected given the retraction of lamellipodia and cell rounding (Fig. 4). Since phosphorylation at Ser239 prevents the anti-capping effects of VASP (Barzik et al., 2005), this suggests that this anti-capping activity of VASP is crucial for its ability to produce lamellipodial spreading. However, given that complete lack of VASP – paradoxically – increases cell speed (Bear et al., 2000), functions other than its anti-capping activity must be important in regulating cell motility – for example by interacting with the substratum. NO does not appear to influence VASP distribution in focal adhesions (Fig. 8) (Smolenski et al., 2000). Loss of lamellipodia with retention of cell adhesion might account for the reduction in cell speed following NO addition.

Phosphorylation of VASP at other amino acid residues also regulates its activity. Phosphorylation of Ser157 produces a substantial conformational change, resulting in altered mobility in SDS-PAGE. Phosphorylation at this site in vivo is largely as a result of PKA activation (Butt et al., 1994). In a study using site-specific mutations of Mena, which has phosphorylation sites homologous to Ser157 and Ser239 of VASP, the equivalent of Ser157 was shown to be essential for VASP function in a motility assay (Loureiro et al., 2002). However, Loureiro and colleagues did not examine the effects of potential activators, such as NO, of phosphorylation equivalent to that of Ser239. Phosphorylation at Thr278 occurs through cAMP-activated protein kinase, and impairs actin-stress-fibre formation and alters cell morphology (Blume et al., 2007). NO had only small effects on Ser157 phosphorylation (Fig. 3a); its effect on Thr278 is not known. Phosphorylation at these sites might also contribute to alterations in VASP distribution and cell motility. However, we have clearly demonstrated here the important effect that NO-dependent phosphorylation of Ser239 has on distribution of VASP, cell shape and motility. The human PTECs used in this study also express, in addition to VASP, Mena and EVL (data not shown), but as our studies were performed using transfected VASP constructs fused to GFP, we cannot make any conclusions as to the possible control of Mena or EVL function by phosphorylation.

We have tested the hypothesis that Ser239 phosphorylation of VASP affects lamellipodial structure and function. We have demonstrated that NO-induced phosphorylation at this site removes VASP from the lamellipodial edge, and leads to retraction of lamellipodia and cell rounding. This is an important means of controlling VASP activity and, hence, potentially regulating actin-based processes, such as directed cell motility.

Materials and Methods

Materials

The NO donor spermine NONOate [N-(2-aminoethyl)-N-(2-hydroxy-2-nitrosohydrazinol-1-2-ethylenediamine)] and the guanylate cyclase inhibitor ODQ (1H-[1,2,4]oxadiazolo [4,3-a]quinoxalin-1-one) were from Calbiochem. Rabbit anti-VASP (M4) was from Alexis Biochemicals. Mouse anti-phosphorylated VASP (Ser239) antibody, clone 16C2, was from Chemicon. Rabbit anti-PKG I (sc-25229) and anti-PKG II (sc-25430) antibodies were from Santa Cruz Biotechnology. Anti-actin antibody was from Abcam. Biotinylated anti-rabbit and anti-mouse antibodies were from Vector Laboratories. Alexa-Fluor-488-conjugated phalloidin and Texas-Red-X-conjugated phalloidin were from Molecular Probes.

Cell culture

Human PTECs were harvested from surgical specimens of human kidneys, obtained under Institutional and National ethical procedures. Isolation and culture of these cells was as described (Glynne et al., 2002; Glynne et al., 2001). Stimulation with cytokines was performed with interleukin-1, tumor necrosis factor and interferon γ exactly as described (Glynne et al., 2001). Human embryonic keratinocytes were obtained from Lonza Biologics (Slough, UK) and grown in media as supplied by the manufacturer.

Plasmids and transfection

cDNA of WT VASP, and of sequences of mutated S239A VASP and S239D VASP were cloned in-frame to the C-terminus of GFP in the vector pQBI25f (QBiogene), using the restriction sites of *Bam*HI and *Eco*RI (resulting in constructs WT GFP-VASP, and S239A GFP-VASP and S239D GFP-VASP, respectively). Human PTECs were transfected using the AMAXA 2 system (AMAXA, Germany), with the basic epithelial transfection kit and programme T-13 and HEKs with the kit specific for these cells. Typically, 1×10^6 cells were transfected with 1 μg of plasmid and then used for imaging ~16 hours later.

Imaging and analysis

For live cell imaging, transfected cells were plated in 2-well glass microscope-chamber slides, maintained in medium containing HEPES. Cells were imaged on a warmed (37°C) stage using a Zeiss Axiovert Inverted Fluorescent Microscope, with ×63 PlanFluor objective and a digital CCD camera (Hamamatsu C4742-95-12ER).

Once a suitable field of view had been chosen, cells were imaged for at least 30 minutes prior to any experimental additions. Where indicated, spermine NONOate was added to a final concentration of 200 μM, following which cells were imaged for at least another 30 minutes. Decomposed NO donor was without effect.

Time-lapse images were acquired using computer-driven shutters and Openlab 5.0 software (Improvision); images were acquired every 30 seconds. Image analysis was performed using Image J (Rasband, W.S., ImageJ, U.S. National Institutes of Health, Bethesda, MA, http://rsb.info.nih.gov/ij/, 1997-2006). Cell speeds were calculated by using the cell outliner Plugin of Image J and measuring the rate of displacement of the cell centroid. To quantify changes following NO donor addition, mean cell speeds 30 minutes prior to donor addition were compared with mean speeds 20 minutes afterwards and expressed as a percentage change. Kymographic analysis of cell movement (Hinz et al., 1999) was performed using plug-ins provided by J. Rietdorf and A. Seitz, EMBL Heidelberg (http://www.embl.de/eamnet/html/kymograph.html). The area of the lamellipodial edge occupied by GFP-VASP was performed using Image J. This was calculated by measuring the area of the edge of all lamellipodia that contained a signal from GFP-VASP (more than five times of background intensity) at various time points. Results were standardized by expressing the data as percent of the value calculated for a given cell immediately prior to NO donor addition. This allowed effects on different cells with different sizes of lamellipodia to be compared directly. To quantify the effects of the S239D mutation on VASP distribution, we scored a cell as having VASP localized to the lamellipodium if more than 10% of the lamellipodial edge had a signal from VASP that was of more than five times of background intensity. Images were prepared for publication using Adobe Photoshop.

Immunoprecipitation

For immunoprecipitation experiments, cells were washed once with cold PBS and lysed in Phosphosafe extraction buffer (Novogen) for 5 minutes at room temperature. Lysates were cleared by centrifugation and incubated with anti-VASP (1:125) for 60 minutes, rotating at 4°C. After incubation, 50 μl of protein G sepharose was added and the mixtures were rotated for a further 60 minutes at 4°C. The beads were then washed four times in Phosphosafe extraction buffer and finally resuspended in gel loading buffer. The bound proteins were resolved by SDS–PAGE and immunoblotting was performed as described below. The amount of phosphorylated VASP Ser157 at various times after NO addition was quantified as a percentage of total VASP by scanning gels immunoblotted with antibody to total VASP. VASP phosphorylated at Ser157 runs with a lower mobility on SDS PAGE with a molecular mass of 50 kDa compared with 46 kDa for VASP not phosphorylated at Ser157.

Immunoblotting

Protein extracts were separated by SDS-PAGE and transferred to Hybond-P membrane (Amersham). After blotting, the membranes were stained with Ponceau S solution (Sigma). Membranes were blocked with 5% skimmed milk in PBS-T (1×PBS with 0.1% Tween-20) and processed for enhanced chemiluminescence by standard methods.

siRNA

The knockdown of PKG I and PKG II were performed using Custom Stealth™ Duplex RNAi (Invitrogen) directed against PKG I nucleotides 1100-1124 and PKG II nucleotides 1344-1368. The RNAi oligonucleotides were transiently transfected in human PTECs using the AMAXA 2 system, as previously described. The relative knockdown efficiency was determined using antibodies against both PKG I and PKG II. A non-specific oligonucleotide was used as a negative control (Ambion).

Statistics

Comparison between two groups was made using Student's *t*-test, two-tailed, unequal variances, with data having a normal distribution by Shapiro-Wilk test. Changes in cell speed following NO donor addition were tested for a difference from zero change using a one-sample *t*-test. For comparisons between larger numbers of groups, analysis of variance was used. For clearly skewed data, comparisons were made using the Mann-Whitney test. The differences in the proportion of lamellipodia containing WT GFP-VASP or S239A GFP-VASP were tested by Fisher's exact test. In all cases, a result was considered significant if $P<0.05$. Statistical testing and curve fitting was performed using the computer program Prism 4.0 (GraphPad).

The work was supported by the Dr Hadwen Trust for Humane Research and the Wellcome Trust (to T.J.E.) and the Deutsche Forschungsgemeinschaft SFB688 (to T.R.).

References

Bachmann, C., Fischer, L., Walter, U. and Reinhard, M. (1999). The EVH2 domain of the vasodilator-stimulated phosphoprotein mediates tetramerization, F-actin binding, and actin bundle formation. *J. Biol. Chem.* **274**, 23549-23557.

Barzik, M., Kotova, T. I., Higgs, H. N., Hazelwood, L., Hanein, D., Gertler, F. B. and Schafer, D. A. (2005). Ena/VASP proteins enhance actin polymerization in the presence of barbed end capping proteins. *J. Biol. Chem.* **280**, 28653-28662.

Bear, J. E., Loureiro, J. J., Libova, I., Fassler, R., Wehland, J. and Gertler, F. B. (2000). Negative regulation of fibroblast motility by Ena/VASP proteins. *Cell* **101**, 717-728.

Bear, J. E., Svitkina, T. M., Krause, M., Schafer, D. A., Loureiro, J. J., Strasser, G. A., Maly, I. V., Chaga, O. Y., Cooper, J. A., Borisy, G. G. et al. (2002). Antagonism between Ena/VASP proteins and actin filament capping regulates fibroblast motility. *Cell* **109**, 509-521.

Bicker, G. (2005). STOP and GO with NO: nitric oxide as a regulator of cell motility in simple brains. *BioEssays* **27**, 495-505.

Blume, C., Benz, P. M., Walter, U., Ha, J., Kemp, B. E. and Renne, T. (2007). AMP-activated protein kinase impairs endothelial actin cytoskeleton assembly by phosphorylating vasodilator-stimulated phosphoprotein. *J. Biol. Chem.* **282**, 4601-4612.

Bretschneider, T., Diez, S., Anderson, K., Heuser, J., Clarke, M., Muller-Taubenberger, A., Kohler, J. and Gerisch, G. (2004). Dynamic actin patterns and Arp2/3 assembly at the substrate-attached surface of motile cells. *Curr. Biol.* **14**, 1-10.

Butt, E., Abel, K., Krieger, M., Palm, D., Hoppe, V., Hoppe, J. and Walter, U. (1994). cAMP- and cGMP-dependent protein kinase phosphorylation sites of the focal adhesion vasodilator-stimulated phosphoprotein (VASP) in vitro and in intact human platelets. *J. Biol. Chem.* **269**, 14509-14517.

Coppolino, M. G., Krause, M., Hagendorff, P., Monner, D. A., Trimble, W., Grinstein, S., Wehland, J. and Sechi, A. S. (2001). Evidence for a molecular complex consisting of Fyb/SLAP, SLP-76, Nck, VASP and WASP that links the actin cytoskeleton to Fcgamma receptor signalling during phagocytosis. *J. Cell Sci.* **114**, 4307-4318.

Diez, S., Gerisch, G., Anderson, K., Muller-Taubenberger, A. and Bretschneider, T. (2005). Subsecond reorganization of the actin network in cell motility and chemotaxis. *Proc. Natl. Acad. Sci. USA* **102**, 7601-7606.

Glynne, P. A., Picot, J. and Evans, T. J. (2001). Co-expressed nitric oxide synthase and apical β_1 integrins influence tubule cell adhesion following cytokine injury. *J. Am. Soc. Nephrol.* **12**, 2370-2383.

Glynne, P. A., Darling, K. E., Picot, J. and Evans, T. J. (2002). Epithelial inducible nitric-oxide synthase is an apical EBP50-binding protein that directs vectorial nitric oxide output. *J. Biol. Chem.* **277**, 33132-33138.

Haase, A. and Bicker, G. (2003). Nitric oxide and cyclic nucleotides are regulators of neuronal migration in an insect embryo. *Development* **130**, 3977-3987.

Harbeck, B., Huttelmaier, S., Schluter, K., Jockusch, B. M. and Illenberger, S. (2000). Phosphorylation of the vasodilator-stimulated phosphoprotein regulates its interaction with actin. *J. Biol. Chem.* **275**, 30817-30825.

Hinz, B., Alt, W., Johnen, C., Herzog, V. and Kaiser, H. W. (1999). Quantifying lamella dynamics of cultured cells by SACED, a new computer-assisted motion analysis. *Exp. Cell Res.* **251**, 234-243.

Hofmann, F., Ammendola, A. and Schlossmann, J. (2000). Rising behind NO: cGMP-dependent protein kinases. *J. Cell Sci.* **113**, 1671-1676.

Huttelmaier, S., Harbeck, B., Steffens, O., Messerschmidt, T., Illenberger, S. and Jockusch, B. M. (1999). Characterization of the actin binding properties of the vasodilator-stimulated phosphoprotein VASP. *FEBS Lett.* **451**, 68-74.

Jay, D. G. (2000). The clutch hypothesis revisited: ascribing the roles of actin-associated proteins in filopodial protrusion in the nerve growth cone. *J. Neurobiol.* **44**, 114-125.

Krause, M., Sechi, A. S., Konradt, M., Monner, D., Gertler, F. B. and Wehland, J. (2000). Fyn-binding protein (Fyb)/SLP-76-associated protein (SLAP), Ena/vasodilator-stimulated phosphoprotein (VASP) proteins and the Arp2/3 complex link T cell receptor (TCR) signaling to the actin cytoskeleton. *J. Cell Biol.* **149**, 181-194.

Krause, M., Dent, E. W., Bear, J. E., Loureiro, J. J. and Gertler, F. B. (2003). Ena/VASP proteins: regulators of the actin cytoskeleton and cell migration. *Annu. Rev. Cell Dev. Biol.* **19**, 541-564.

Krause, M., Leslie, J. D., Stewart, M., Lafuente, E. M., Valderrama, F., Jagannathan, R., Strasser, G. A., Rubinson, D. A., Liu, H., Way, M. et al. (2004). Lamellipodin, an Ena/VASP ligand, is implicated in the regulation of lamellipodial dynamics. *Dev. Cell* **7**, 571-583.

Lambrechts, A., Kwiatkowski, A. V., Lanier, L. M., Bear, J. E., Vandekerckhove, J., Ampe, C. and Gertler, F. B. (2000). cAMP-dependent protein kinase phosphorylation of EVL, a Mena/VASP relative, regulates its interaction with actin and SH3 domains. *J. Biol. Chem.* **275**, 36143-36151.

Laurent, V., Loisel, T. P., Harbeck, B., Wehman, A., Grobe, L., Jockusch, B. M., Wehland, J., Gertler, F. B. and Carlier, M. F. (1999). Role of proteins of the Ena/VASP family in actin-based motility of Listeria monocytogenes. *J. Cell Biol.* **144**, 1245-1258.

Lawrence, D. W. and Pryzwansky, K. B. (2001). The vasodilator-stimulated phosphoprotein is regulated by cyclic gmp-dependent protein kinase during neutrophil spreading. *J. Immunol.* **166**, 5550-5556.

Lebrand, C., Dent, E. W., Strasser, G. A., Lanier, L. M., Krause, M., Svitkina, T. M., Borisy, G. G. and Gertler, F. B. (2004). Critical role of Ena/VASP proteins for filopodia formation in neurons and in function downstream of netrin-1. *Neuron* **42**, 37-49.

Lee, Y. C., Martin, E. and Murad, F. (2000). Human recombinant soluble guanylyl cyclase: expression, purification, and regulation. *Proc. Natl. Acad. Sci. USA* **97**, 10763-10768.

Loureiro, J. J., Rubinson, D. A., Bear, J. E., Baltus, G. A., Kwiatkowski, A. V. and Gertler, F. B. (2002). Critical roles of phosphorylation and actin binding motifs, but not the central proline-rich region, for Ena/vasodilator-stimulated phosphoprotein (VASP) function during cell migration. *Mol. Biol. Cell* **13**, 2533-2546.

Mejillano, M. R., Kojima, S., Applewhite, D. A., Gertler, F. B., Svitkina, T. M. and Borisy, G. G. (2004). Lamellipodial versus filopodial mode of the actin nanomachinery: pivotal role of the filament barbed end. *Cell* **118**, 363-373.

Murohara, T., Witzenbichler, B., Spyridopoulos, I., Asahara, T., Ding, B., Sullivan, A., Losordo, D. W. and Isner, J. M. (1999). Role of endothelial nitric oxide synthase in endothelial cell migration. *Arterioscler. Thromb. Vasc. Biol.* **19**, 1156-1161.

Oelze, M., Mollnau, H., Hoffmann, N., Warnholtz, A., Bodenschatz, M., Smolenski, A., Walter, U., Skatchkov, M., Meinertz, T. and Munzel, T. (2000). Vasodilator-stimulated phosphoprotein serine 239 phosphorylation as a sensitive monitor of defective nitric oxide/cGMP signaling and endothelial dysfunction. *Circ. Res.* **87**, 999-1005.

Pfeifer, A., Aszodi, A., Seidler, U., Ruth, P., Hofmann, F. and Fassler, R. (1996). Intestinal secretory defects and dwarfism in mice lacking cGMP-dependent protein kinase II. *Science* **274**, 2082-2086.

Pfeifer, A., Klatt, P., Massberg, S., Ny, L., Sausbier, M., Hirneiss, C., Wang, G. X., Korth, M., Aszodi, A., Andersson, K. E. et al. (1998). Defective smooth muscle regulation in cGMP kinase I-deficient mice. *EMBO J.* **17**, 3045-3051.

Reinhard, M., Halbrügge, M., Scheer, U., Wiegand, C., Jockusch, B. M. and Walter, U. (1992). The 46/50 kDa phosphoprotein VASP purified from human platelets is a novel protein associated with actin filaments and focal contacts. *EMBO J.* **11**, 2063-2070.

Renfranz, P. J. and Beckerle, M. C. (2002). Doing (F/L)PPPPs: EVH1 domains and their proline-rich partners in cell polarity and migration. *Curr. Opin. Cell Biol.* **14**, 88-103.

Rottner, K., Behrendt, B., Small, J. V. and Wehland, J. (1999). VASP dynamics during lamellipodia protrusion. *Nat. Cell Biol.* **1**, 321-322.

Samarin, S., Romero, S., Kocks, C., Didry, D., Pantaloni, D. and Carlier, M. F. (2003). How VASP enhances actin-based motility. *J. Cell Biol.* **163**, 131-142.

Schirenbeck, A., Arasada, R., Bretschneider, T., Stradal, T. E., Schleicher, M. and Faix, J. (2006). The bundling activity of vasodilator-stimulated phosphoprotein is required for filopodium formation. *Proc. Natl. Acad. Sci. USA* **103**, 7694-7699.

Smolenski, A., Poller, W., Walter, U. and Lohmann, S. M. (2000). Regulation of human endothelial cell focal adhesion sites and migration by cGMP-dependent protein kinase I. *J. Biol. Chem.* **275**, 25723-25732.

Vasioukhin, V. and Fuchs, E. (2001). Actin dynamics and cell-cell adhesion in epithelia. *Curr. Opin. Cell Biol.* **13**, 76-84.

Yaroslavskiy, B. B., Zhang, Y., Kalla, S. E., Garcia Palacios, V., Sharrow, A. C., Li, Y., Zaidi, M., Wu, C. and Blair, H. C. (2005). NO-dependent osteoclast motility: reliance on cGMP-dependent protein kinase I and VASP. *J. Cell Sci.* **118**, 5479-5487.

Zhuang, S., Nguyen, G. T., Chen, Y., Gudi, T., Eigenthaler, M., Jarchau, T., Walter, U., Boss, G. R. and Pilz, R. B. (2004). Vasodilator-stimulated phosphoprotein activation of serum-response element-dependent transcription occurs downstream of RhoA and is inhibited by cGMP-dependent protein kinase phosphorylation. *J. Biol. Chem.* **279**, 10397-10407.

Journal of Cell Science